CrossMark

ORIGINAL PAPER

Calreticulin attenuated microwave radiation-induced human microvascular endothelial cell injury through promoting actin acetylation and polymerization

Feifei Xu [1] · You Wang [1] · Tianqi Tao [1] · Dandan Song [1] · Xiuhua Liu [1,2]

Abstract Recent work reveals that actin acetylation modification has been linked to different normal and disease processes and the effects associated with metabolic and environmental stressors. Herein, we highlight the effects of calreticulin on actin acetylation and cell injury induced by microwave radiation in human microvascular endothelial cell (HMEC). HMEC injury was induced by high-power microwave of different power density (10, 30, 60, 100 mW/cm^2, for 6 min) with or without exogenous recombinant calreticulin. The cell injury was assessed by lactate dehydrogenase (LDH) activity and Cell Counting Kit-8 in culture medium, migration ability, intercellular junction, and cytoskeleton staining in HMEC. Western blotting analysis was used to detected calreticulin expression in cytosol and nucleus and acetylation of globular actin (G-actin). We found that HMEC injury was induced by microwave radiation in a dose-dependent manner. Pretreatment HMEC with calreticulin suppressed microwave radiation-induced LDH leakage and increased cell viability and improved microwave radiation-induced decrease in migration, intercellular junction, and cytoskeleton. Meanwhile, pretreatment HMEC with exogenous calreticulin upregulated the histone acetyltransferase activity and the acetylation level of G-actin and increased the fibrous actin (F-actin)/G-actin ratio. We conclude that exogenous calreticulin protects HMEC against microwave radiation-induced injury through promoting actin acetylation and polymerization.

Keywords Calreticulin · Human microvascular endothelial cell · Actin acetylation · Microwave radiation

Co-first authors Fei-Fei Xu and You Wang contributed equally to this work.

✉ Xiuhua Liu
xiuhualiu98@163.com

[1] Department of Pathophysiology, Chinese PLA General Hospital, Beijing, China

[2] State Key Laboratory of Kidney Disease, Chinese PLA General Hospital, Beijing, China

Introduction

With the advent of wireless technology, there has been a massive increase of electromagnetic radiation exposure to human beings from microwaves to radiowaves and other invisible radiation. It has been known that certain intensities of microwave radiation, especially high-power microwave (HPM), could damage multiple organs (Sanders et al. 1984; Kantz et al. 2005; Zhao et al. 2012; K Sri 2015). However, the prevention and treatment of HPM-induced injury remain elusive. Microvessels are pivotal for maintaining the physiological functions of tissues and organs (Secomb and Pries 2011). A restricted or defective microvascular endothelia function is the cause of a number of health complaints and illnesses. Several studies have reported that microwave radiation leads to capillary malformation, slows blood flow, and decreases the arterial and venous diameters of capillary loop (Li et al. 1997), and microwave energy increases testis microvascular permeability (Gao et al. 2008). Our previous work mainly focused on the effect of different frequency microwave on the microvascular endothelial cells and found that microwave, served as stressor, induces endoplasmic reticulum (ER) stress of HMEC and the intensity of stress is dose-dependently (Li et al. 2014b). We also found that one of the ER stress proteins, calreticulin, has the protective effect to inhibit HPM-induced cell injury and determined the effective concentration and action time (Li et al. 2014a).

Calreticulin (CRT) is an endoplasmic reticulum luminal Ca^{2+}-binding protein and a molecular chaperone. Previous studies mainly focused on its regulation on protein folding and calcium homeostasis (Michalak et al. 2009). In recent years, it has been reported that CRT also exists in the surface of cell membrane, cytoplasm, nucleus, and extracellular matrix, known as "non-endoplasmic reticulum calreticulin," regulating cell proliferation, adhesion, migration, and apoptosis and involving in cancer, cardiocerebrovascular diseases, and diabetes (Gold et al. 2010). The potential therapeutic effects of exogenous calreticulin on cancer, ischemic diseases, and chronic wound healing have become one of the medical research hotspots (Wang et al. 2012a; Riahi et al. 2010; Haseloff et al. 2006). Our previous work confirmed that overexpression of cytoplasmic calreticulin (Xu et al. 2014) or pretreatment of exogenous recombinant calreticulin (Li et al. 2014a) relieved F-actin malalignment and microfilament rupture. However, the mechanisms underlying needed to be clarified.

Cytoplasmic actin is essential for the survival of endothelial cells: provides internal mechanical structure and motility and maintains asymmetrical shapes for cells (Pollard and Cooper 2009). Under physiological conditions, G-actin polymerizes into F-actin with a helical arrangement of subunits. Accumulating evidence suggests that actin acetylation regulates the monomer–polymer equilibrium and organization of actin and plays important roles in modulating actin's regulation role in cell survival, movement, intracellular transport, and direct pathological processes (Terman and Kashina 2013). Previous studies have reported that calreticulin has acetyl transferase activity, using 7,8-diacetoxy-4-methylcoumarin (DAMC) or acetyl-CoA as substrates, transferring the acetyl group to receptor proteins such as triphosphopyridine nucleotide (NADPH), cytochrome C reductase (CYPR), and neuronal nitric oxide synthase (nNOS) and regulating the spatial structure and functional activity of the receptor proteins (Seema et al. 2007; Singh et al. 2011).

To investigate the effect of S-band microwave of different power densities on the morphology and function of microvascular endothelial cell, we used the radiation injury model of HMEC induced by high-power microwave of different power densities and observed the LDH activity in culture medium, endothelial cell migration, viability, VE-cadherin, and cytoskeleton immunofluorescent staining, to reflect the injury of HMEC induced by microwave radiation (MR). Based on these results, we chose the microwave power density which could cause obvious functional and morphological injury of endothelial cells and added exogenous recombinant calreticulin for pretreatment 20 min before MR to investigate the protective effect of CRT on actin acetylation, cytoskeleton stability, and endothelial function to against MR injury.

Materials and methods

Antibodies and reagents

Endothelial cell medium (ECM) was purchased from Sciencell (Carlsbad, CA); trypsin was purchased from Amresco (Solon, OH, USA). The protease inhibitor, penicillin/streptomycin, Triton X-100, and phalloidin-FITC were purchased from Sigma (St. Louis, MO, USA). Rabbit polyclonal antibodies against calreticulin, Pan-actin, acetylated lysine, GAPDH, or histone H3 were purchased from Cell Signaling Technology (Danvers, MA, USA). Human CRT recombinant protein (10-288-22432F) was obtained from GenWay Biotech, Inc. (San Diego, CA, USA). Rabbit polyclonal antibody against VE-cadherin-FITC was purchased from Abcam (Cambridge, UK). Phosphatase inhibitor and bovine serum albumin (BSA) were purchased from Merck (Rahway, NJ, USA). The Annexin V/FITC Apoptosis Direction Kit and the Cell Counting Kit-8 (CCK-8) detection kit were from Kaiji Biological Engineering Company (Nanjing, China). The lactate dehydrogenase (LDH) detection kit was purchased from Nanjing Jiancheng Biological Engineering Institute (Nanjing, China). The HAT Activity Colorimetric Assay Kit and the Nuclear/Cytosol Fractionation Kit were purchased from BioVision Incorporated (Milpitas, CA, USA). The enhanced chemiluminescence kit was purchased from Santa Cruz Biotechnology (Santa Cruz, CA, USA). The horseradish peroxidase (HRP)-conjugated goat anti-rabbit immunoglobulin G (IgG) was purchased from Epitomics (Burlingame, CA, USA).

Cell culture and experiment protocol

The HMEC was purchased from the Institute of Biomedical Sciences (IBS), Fudan University and cultured as described previously (Bender et al. 2008). During the logarithmic phase of culture, HMEC cells were transferred to serum-low maintenance medium (ECM with 1% FCS and 1% penicillin/streptomycin) for 12 h and randomized to carry out the following two parts of the experiment as described previously (Li et al. 2014b; Li et al. 2014a; Xu et al. 2014) (each experiment had been repeated for three times independently, $n = 3$).

Part I. To assess the effect of different power density MR on the morphology and function of HMEC and the acetylation and polymerization status of actin, cells were divided into five groups: (1) control group (control): HMEC cells remained in a 5% CO_2 incubator at 37 °C for the duration of the experiment; (2)–(5) MR groups: cells were exposed to MR of different power densities as 10 mW/cm^2 (10 mW), 30 mW/cm^2 (30 mW), 60 mW/cm^2 (60 mW), and 100 mW/cm^2 (100 mW) for 6 min and then returned to the 5%

CO_2 incubator at 37 °C for 24 h. The temperature changes induced by microwave radiation for 6 min are within the temperature range for cell normal growth (Li et al. 2014b; Li et al. 2014a; Xu et al. 2014).

Part II. To assess the effect of calreticulin on the HMEC injury induced by MR and the acetylation and polymerization status of actin, cells were divided into four groups: (1) control group (control): HMEC cells remained in a 5% CO_2 incubator at 37 °C for the duration of the experiment; (2) CRT group (CRT): the normal cultured cells were incubated with exogenous CRT (25 pg/mL) for 24 h; (3) microwave radiation group (60 mW): cells were exposed to MR of 60 mW/cm^2 for 6 min and then returned to the 5% CO_2 incubator at 37 °C for 24 h; (4) CRT + MR group (CRT + 60 mW): cells were incubated with CRT (25 pg/mL) for 20 min before radiation and then treated as group (3) described above.

Detection of cell injury and viability

LDH activity was assessed in culture medium using an LDH assay kit to estimate LDH leakage under various treatment conditions. CCK-8 detection was an alternative method used for estimating cell viability. This measures metabolic activity through the ability of the cells to convert tetrazolium dye to its insoluble form, formazan (Hou et al. 2007). Cells were seeded and plated in 96-well plates and then incubated with CCK-8 for 4 h. Samples were measured using a microplate reader at 450 nm wavelength (Tecan Infinite f200 Pro; Tecan Group Ltd., Männedorf, Switzerland).

Endothelial cell migration

The endothelial cell migration ability was determined by the scratch wound assay, as reported previously (Vicari et al. 2011). Briefly, cells were seeded in 24-well plates precoated with 0.1% gelatin. Upon reaching confluence, cells were cultured in serum-low medium overnight. Then, a 3-mm-wide scratch wound was created by scraping the monolayer of cells with a sterile pipet tip. Cellular debris was washed out by using culture medium, and cells were exposed to MR for 6 min and then returned to the 5% CO_2 incubator at 37 °C for 24 h. After treatment, the cells were fixed and micrographs were captured with an inverted bright-field microscope (×400 magnifications). Cell migration toward the scratch wound was quantified with Image-Pro Plus software.

Immunofluorescence staining

HMEC cells were grown on coverslips and fixed using 4% paraformaldehyde at room temperature for 25 min. They were then blocked in phosphate-buffered saline containing 10% donkey serum, 1% BSA, and 0.1% Triton X-100 for 50 min. The intercellular junction was identified by direct immunofluorescence staining using FITC-anti-VE-cadherin rabbit polyclonal antibody for 2 h in the dark at room temperature. For F-actin detection, cells were stained in the dark at room temperature for 1 h with phalloidin-FITC at a final concentration of 0.33 μmol/L (Wang et al. 2012b, 2014). The coverslips were mounted on glass slides with mounting medium. Images were acquired using a confocal scanning microscope (Zeiss LSM-510 Meta, Jena, Germany), and a 63× oil immersion objective with a numerical aperture of 1.4 was used.

Histone acetyltransferase activity assay of subcellular components

The histone acetyltransferase activity of cytosol and nuclear extract samples was tested using the HAT Activity Colorimetric Assay Kit, which utilizes active nuclear extract (NE) as a positive control and acetyl-CoA as a cofactor. Acetylation of peptide substrate by active HAT releases the free form of CoA which then serves as an essential coenzyme for producing NADH. NADH can easily be detected spectrophotometrically upon reacting with a soluble tetrazolium dye. The extract should be prepared using the Nuclear/Cytosol Fractionation Kit without DTT. The samples (50 μg of nuclear or cytosol extracts) in 40 μL water (final volume) for each assay in a 96-well plate were tested according to the protocol using a microplate reader at 440 nm wavelength (Tecan Infinite f200 Pro; Tecan Group Ltd., Männedorf, Switzerland).

Separation of G-actin and F-actin

Cells were plated in 60-mm dishes at 3×10^4 cm^{-2}. After the experiment, cells were lysed with actin stabilization buffer containing 10 mmol/L Tris (pH 7.4), 2 mmol/L $MgCl_2$, 1% Triton X-100, 0.2 mmol/L dithiothreitol, and 15% glycerol. Soluble (G-actin) and insoluble (F-actin) fractions were separated by centrifugation (12,800×g, 1 min) at 4 °C, resolved by 10% SDS-PAGE, and subjected to western blot analysis as previously described (Tao et al. 2015).

Western blot analysis

The protein concentration of subcellular extractions and G-actin or F-actin fractions was detected using Bradford assay. Each fraction was resolved on 10% SDS-PAGE using an equal amount of protein (80 μg/lane). Following

electrophoresis, proteins were electrophoretically transferred to nitrocellulose membranes and then blocked with 5% BSA in Tris-buffered saline containing 0.1% Tween 20 (TBS-T) at room temperature for 1 h. Then, membranes were probed with primary antibodies against calreticulin, Pan-actin, acetylated lysine, GAPDH, and histone 3 (all 1:500 diluted) at 4 °C overnight. The antibody-tagged membranes were incubated with a secondary antibody solution consisting of either a 1:1000 dilution of HRP-conjugated goat anti-rabbit IgG. An enhanced chemiluminescence detection system was used for immunoblot protein detection. Optical densities of the bands were analyzed using Image-Pro Plus software, and the densitometry results were normalized to GAPDH or histone 3.

Coimmunoprecipitation

Coimmunoprecipitation was done using immunoprecipitation kit (Roche, USA) according to manufacturer's instruction. Briefly, HMECs (1×10^6) were incubated with exogenous CRT (25 pg/mL) for 30 min, rinsed with cold PBS, and lysed in 1 mL lysis buffer on ice for 10 min. Cell debris was pelleted at 4 °C 12,000×g for 10 min. Lysates were precleared using protein G-agarose (50 μL) with rotation for 3 h at 4 °C. After centrifugation, protein concentrations were determined by the Bradford procedure. Precleared lysates were incubated with goat anti-CRT antibody (sc-7431, Santa Cruz) 30 μL or mouse anti-actin antibody (NB600-535, NOVUS) 30 μL with rotation for 3 h at 4 °C and then added protein G-agarose (60 μL) with rotation for overnight at 4 °C. After washing with wash buffer, captured immune complexes were eluted using elution buffer and loaded in SDS-PAGE, transferred onto nitrocellulose membrane. Blots were blocked in 0.05% TBS, 20% Tween, and 5% non-fat milk followed by probing with the indicated primary (rabbit anti-Pan-actin, 4968, Cell Signaling Technology, or rabbit anti-CRT, ADI-SPA-600F, Enzo) and secondary antibodies (goat anti-rabbit IgG (H+L)-HRP, ZB-2301, ZSGB-BIO). Immunoreactivity was detected with an enhanced chemiluminiscence system.

Statistical analysis

The SPSS v13.0 program (Chicago, IL, USA) was used for statistical analysis. For multiple-group comparisons, one-way analysis of variance followed by *Newman–Keuls* post hoc analysis was performed. Values are presented as mean ± SD. *Pearson bivariate correlation* analysis was applied to determine the correlation between variables. $P < 0.05$ was considered to be statistically significant.

Results

Effects of CRT on HMEC injury induced by microwave radiation

LDH activity

LDH activity in culture medium was measured to estimate the amount of LDH leakage from HMEC to assess cytomembrane injury (Fig. 1). LDH activity in the culture medium was 29.05 ± 3.65 U/L in control group. When exposed to microwave for the same duration, along with the increase of power density, the cytomembrane injury of HMEC was aggravated gradually as showed by LDH activity in culture medium increased. After exposed to microwave of 10, 30, 60, or 100 mW/cm^2 for 6 min, compared with the control group, the LDH activity increased 269, 622, 761, or 1471%, respectively ($P < 0.05$ vs. control) (Fig. 1a), indicating that MR induces dose-dependent injury of HMEC cytomembrane.

Under the normal condition, incubation with exogenous CRT has no obvious effect of the membrane permeability of HMEC. The LDH activity in medium of CRT group has no significant difference ($P > 0.05$). After MR, compared with control, the LDH activity of 60 mW group and CRT + 60 mW
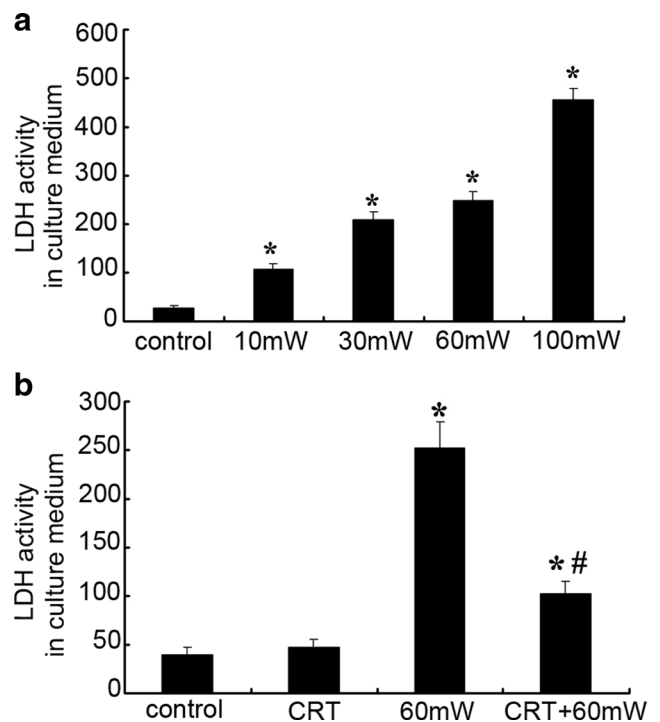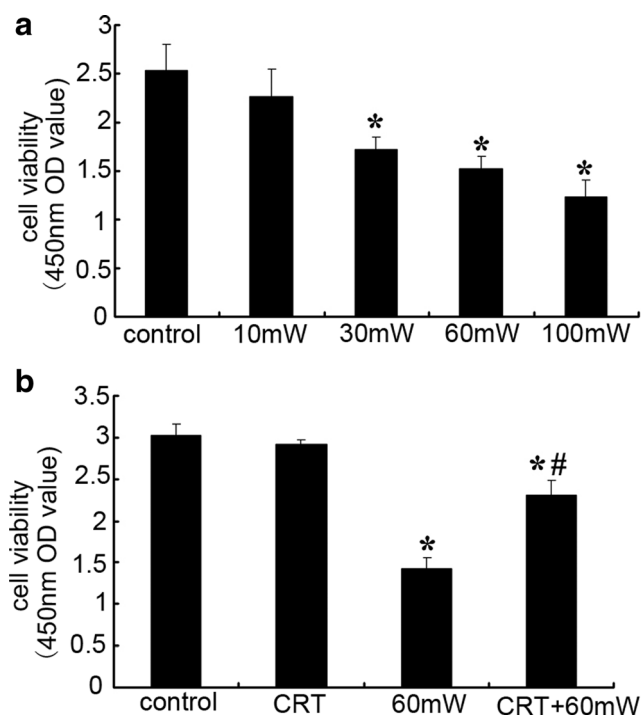

Fig. 1 Calreticulin (CRT) pretreatment reduced the LDH leakage from human microvascular endothelial cell (HMEC) induced by MR. **a** The effect of different power densities of MR (10, 30, 60, or 100 mW/cm^2) on the LDH activity in culture medium. **b** The effect of CRT pretreatment (25 pg/mL, 20 min before radiation) on the LDH leakage induced by MR. Data were quantified from three independent experiments ($n = 3$). *#$P < 0.05$ vs. control

group increased 550 and 160%, respectively ($P < 0.05$). There was statistical difference between 60 mW group and CRT + 60 mW group ($P < 0.05$) (Fig. 1b), indicating that exogenous CRT pretreatment protected the cytomembrane integrity of HMEC from MR-induced injury.

Cell viability

Cell viability detected by CCK-8 is shown in Fig. 2. When exposed to microwave for the same duration, along with the increase of power density, the viability of HMEC decreased gradually. Compared with control group, the cell viability of 10 mW group had no significant difference ($P > 0.05$). After exposure to microwave of 30, 60, or 100 mW/cm^2 for 6 min, the viability decreased 32, 40, or 51%, respectively ($P < 0.05$ vs. control) (Fig. 2a), indicating that MR induced dose-dependent decrease of HMEC viability.

Under the normal condition, incubation HMEC with exogenous CRT has no significant effect on cell viability ($P > 0.05$ vs. control). After microwave radiation, compared with control, the cell viability of 60 mW group and CRT + 60 mW group decreased 47 and 23%, respectively ($P < 0.05$). There was statistical difference between 60 mW group and CRT + 60 mW group ($P < 0.05$) (Fig. 2b), suggesting that exogenous CRT pretreatment suppressed MR-induced decrease in cell viability.
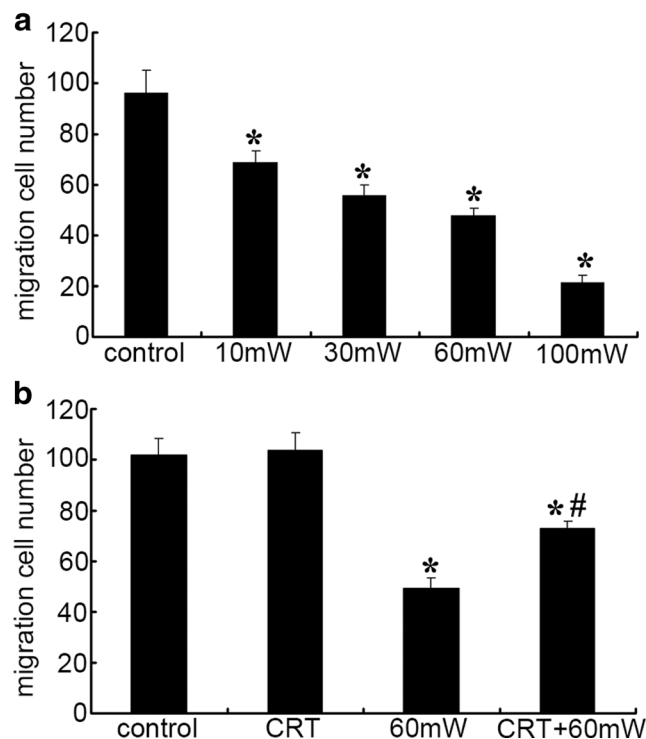
Endothelial cell migration

The migration of vascular endothelial cells plays an important role in the vascular growth and repair of damaged endothelial cells and wounds. It is one of the important parameters to reflect endothelial function (Fig. 3). Compared with control group, the number of migrated cells decreased 29, 42, 50, or 78% in HMEC exposed to microwave of 10, 30, 60, or 100 mW/cm^2 for 6 min, respectively ($P < 0.05$ vs. control) (Fig. 3a), indicating that MR induces dose-dependent decrease of HMEC mobility.

Under the normal condition, pretreatment of the HMEC with exogenous CRT has no obvious effect of the cell mobility ($P > 0.05$ vs. control). After microwave radiation, compared with control, the HMEC mobility of 60 mW group and CRT + 60 mW group decreased 52 and 28%, respectively ($P < 0.05$). There was statistical difference between 60 mW group and CRT + 60 mW group ($P < 0.05$) (Fig. 3b), suggesting that exogenous CRT pretreatment preserves the mobility of HMEC after MR.

Intercellular junction

VE-cadherin is specifically expressed in endothelial cells, which is one of the key factors emerged earliest during the

Fig. 2 The effect of CRT on HMEC viability subjected to MR. **a** The effect of different power densities of MR (10, 30, 60, or 100 mW/cm^2) on the cell viability of HMEC. **b** The effect of CRT pretreatment (25 pg/mL, 20 min before radiation) on the cell viability of HMEC. Data were quantified from three independent experiments ($n = 3$). *#$P < 0.05$ vs. control

Fig. 3 The effect of CRT on cell mobility of HMEC subjected to MR. **a** The effect of different power densities of MR (10, 30, 60, or 100 mW/cm^2) on the cell mobility of HMEC. **b** The effect of CRT pretreatment (25 pg/mL, 20 min before radiation) on the cell mobility of HMEC. Data were quantified from three independent experiments ($n = 3$). *#$P < 0.05$ vs. control

formation of intercellular junction. Using immunofluoresence technique to detect the expression of VE-cadherin might reflect the formation of intercellular junction (Fig. 4). When exposed to microwave for the same duration, along with the increase of power density, the continuity of VE-cadherin was damaged gradually. The fluorescence intensity was weakened and distributed as discontinuous spot (Fig. 4a), suggesting that MR induces dose-dependent damage of the continuity of intercellular adhesion molecule VE-cadherin.

Under the normal condition, incubation with exogenous CRT has no significant effect of the continuity of VE-cadherin compared with control. After MR of 60 mW/cm^2, the continuity of VE-cadherin was damaged, presented the discontinuous punctiform or linear expression of VE-cadherin, and weakened fluorescence in HMEC membrane. CRT pretreatment before radiation helped maintain the fluorescence intensity and continuity of VE-cadherin (Fig. 4b), suggesting that exogenous CRT pretreatment protects the damage of intercellular junction of HMEC induced by MR.

Cytoskeleton staining

We examined cytoskeleton structure by staining the HMEC with phalloidin-FITC, which bound only to F-actin (Fig. 5). The fluorescence microphotographs revealed that in control HMEC, F-actin predominantly appeared as homogenous and continuous stress fibers. When exposed to microwave for the same duration, along with the increase of power density, the cytoskeleton structure was damaged gradually. The fiber bundle arrangement became disordered and ruptured (Fig. 5a), suggesting that MR induces dose-dependent disorganization of F-actin and cytoskeleton damage of the HMEC.

Under the normal condition, incubation with exogenous CRT has no significant effect of the cytoskeleton structure compared with control. After MR of 60 mW/cm^2, F-actin appeared predominantly disorganized with scattered ruptures. CRT pretreatment before radiation helped maintain the fiber bundle arrangement of microfilament cytoskeleton and increased the fluorescence intensity of fiber bundles (Fig. 5b), suggesting that exogenous CRT pretreatment helps maintain cytoskeleton structure and improve cytoskeleton remodeling and disarrangement of HMEC induced by MR.

Effects of CRT pretreatment on CRT expression and the histone acetyltransferase activity of cytosol and nuclear extracts

After verifying that CRT pretreatment protects the functional and morphological injury of HMEC induced by MR, we further investigated the effect of CRT pretreatment before radiation on the intracellular distribution of CRT and the histone acetyltransferase activity of cytosol and nuclear extracts (Fig. 6).
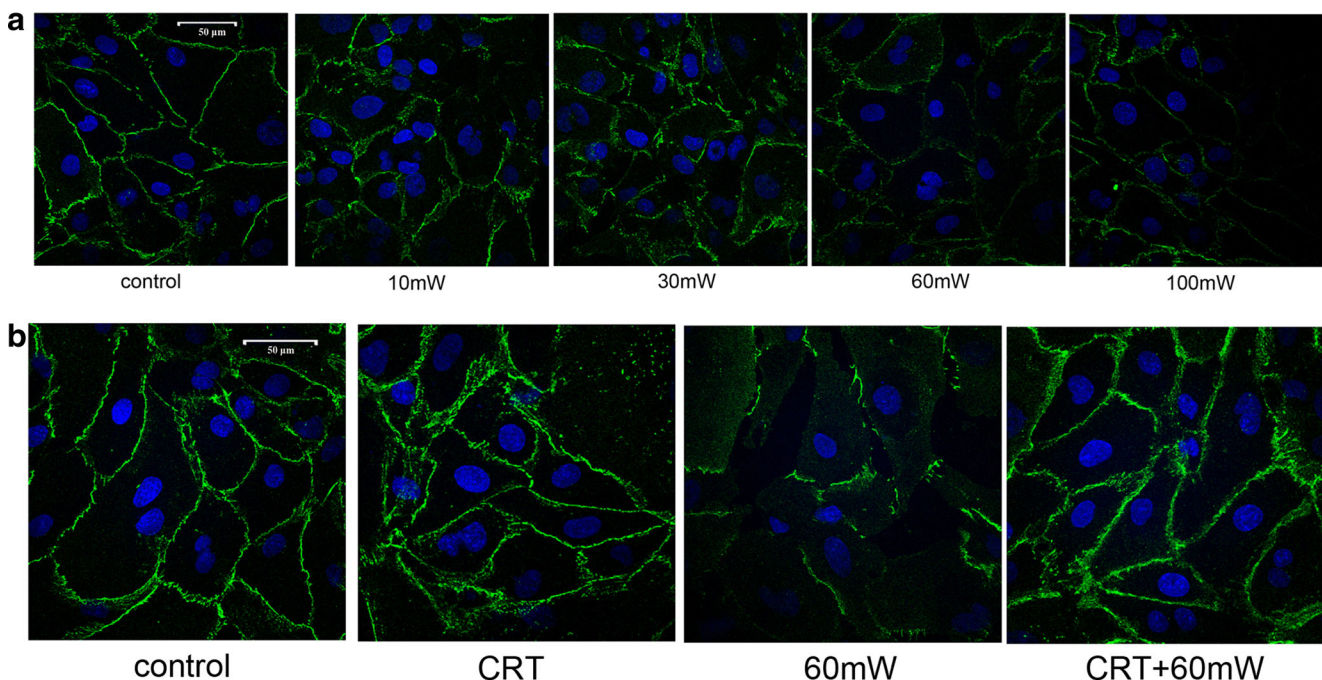
Fig. 4 The effect of CRT on the VE-cadherin continuity of HMEC subjected to MR. The immunofluorescence staining of FITC-VE-cadherin was used to analyze the spatial distribution of VE-cadherin. **a** The effect of different power densities of MR (10, 30, 60, or 100 mW/cm^2) on the distribution of VE-cadherin of HMEC. **b** The effect of CRT pretreatment (25 pg/mL, 20 min before radiation) on the distribution of VE-cadherin of HMEC. Samples were examined by confocal laser scanning microscopy. *Scale bar* is 50 μm. Experiments were done in triplicate ($n = 3$), and representative images are presented
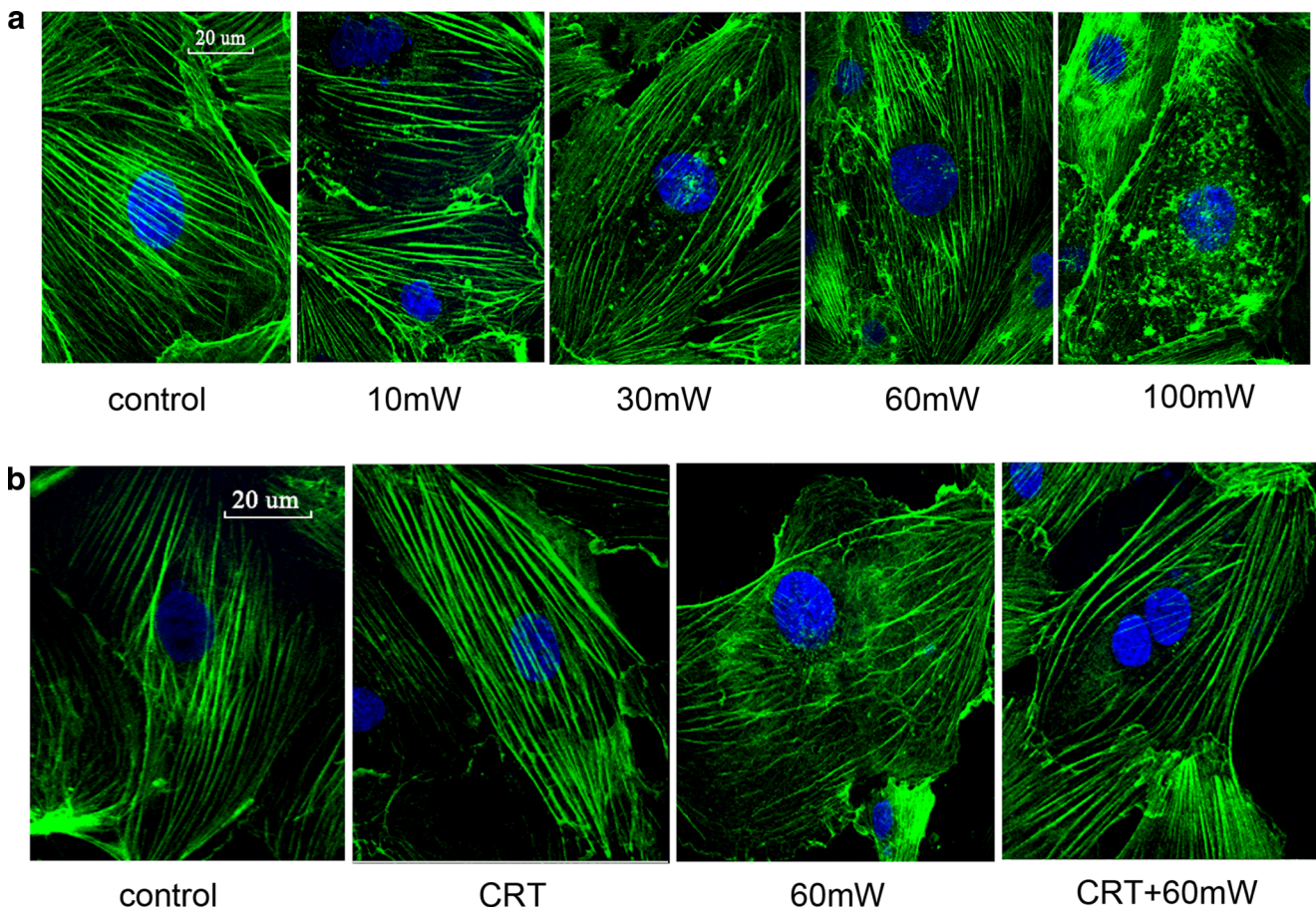
Fig. 5 The effect of CRT on the cytoskeleton structure of HMEC subjected to MR. FITC-phalloidin was used to label and analyze the spatial distribution of F-actin. **a** The effect of different power densities of MR (10, 30, 60, or 100 mW/cm^2) on the cytoskeleton structure of HMEC. **b** The effect of CRT pretreatment (25 pg/mL, 20 min before radiation) on the cytoskeleton structure of HMEC. Samples were examined by confocal laser scanning microscopy. *Scale bar* is 20 μm. Experiments were done in triplicate ($n = 3$), and representative images are presented

We separated the protein components of cytosol and nucleus and used western blotting to detect the relative expression of CRT in different components. The relative expression of CRT in cytosol was calibrated by GAPDH as internal reference, while it was calibrated by histone 3 in nucleus (Fig. 6a). After microwave radiation, in cytosol, the CRT relative expression of 60 mW group decreased 17.8% ($P < 0.05$), while that of CRT + 60 mW group increased 9.9% ($P > 0.05$) compared with control. In nucleus, the CRT relative expression of 60 mW group increase 94.4% ($P < 0.05$), and that of CRT + 60 mW group increased 27.2% ($P < 0.05$) compared with control. There was statistical difference between 60 mW group and CRT + 60 mW group ($P < 0.05$) (Fig. 6b), suggesting that exogenous CRT pretreatment might prevent the relocalization of CRT from cytosol to nucleus.

The histone acetyltransferase activity of cytosol and nuclear extract samples was tested using the HAT Activity Colorimetric Assay Kit (Biovision) (Fig. 6c). Acetyl-CoA is a substrate for a large group of HATs. In our study, we standardized the experimental conditions of different groups and then measured the relative changes in acetyl transferase activity contributing to the changes in CRT activity. After microwave radiation, in cytosol, the HAT activity of 60 mW group decreased 22% ($P < 0.05$), while that of CRT + 60 mW group increased 25.8% ($P < 0.05$) compared with control. In nucleus, the HAT activity of 60 mW group increased 30% ($P < 0.05$), and that of CRT + 60 mW group increased 9.0% ($P > 0.05$) compared with control. There was statistical difference between 60 mW group and CRT + 60 mW group ($P < 0.05$) (Fig. 6c), suggesting that high-power microwave induced CRT nuclear translocation of HMEC, and exogenous CRT pretreatment preserved the HAT activity in cytosol, and it might preserve G-actin acetylation and stabilize the polymerization status of microfilaments.

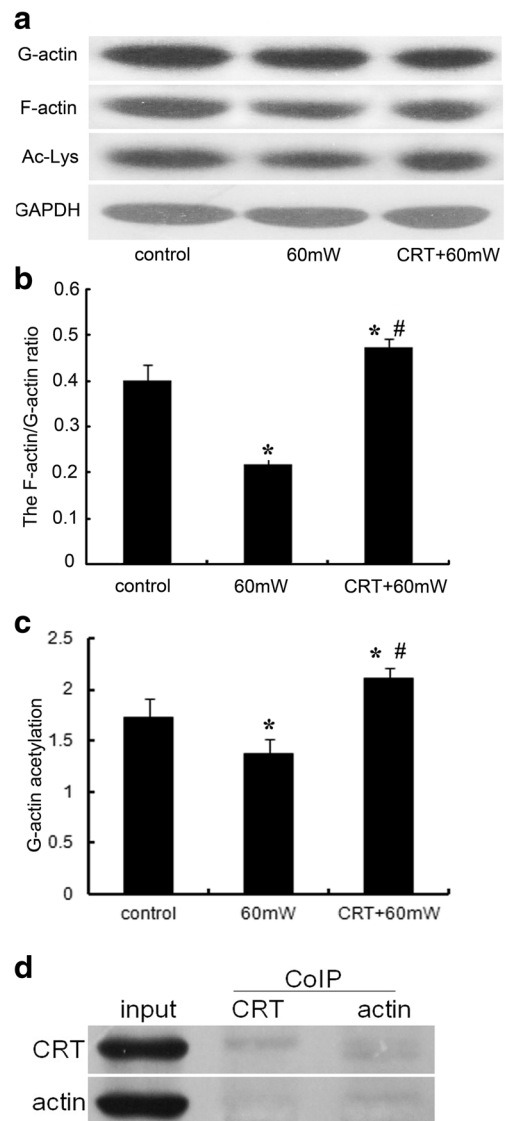### Effects of CRT on the F-actin/G-actin ratio and acetylation of G-actin

Actin polymerization is critical for cell shape and many regulatory responses including endothelial cell migration,
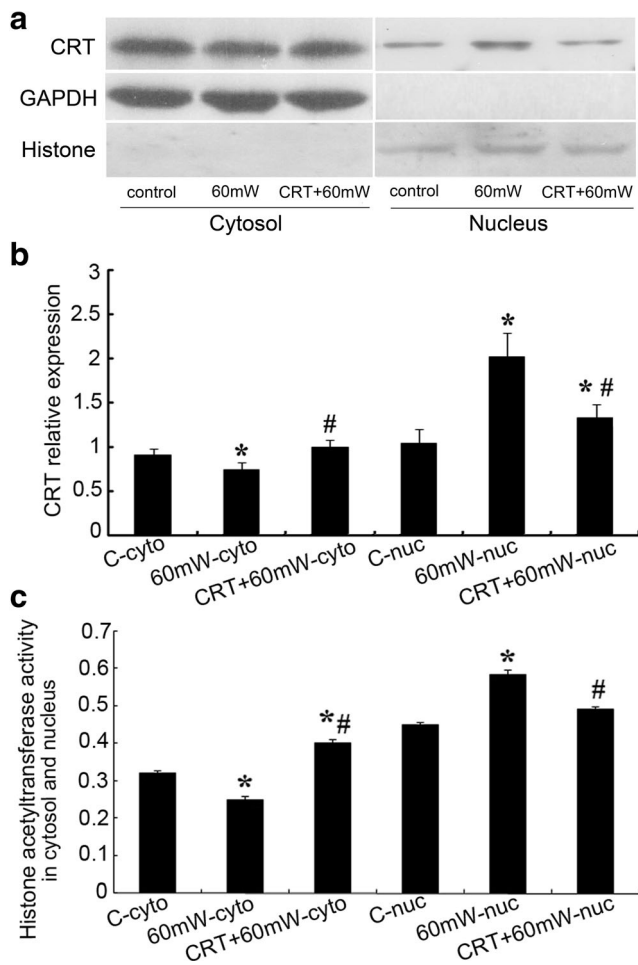
Fig. 6 The effect of CRT on the CRT expression and the histone acetyltransferase activity of cytosol and nuclear extracts of HMEC subjected to MR. **a** The cytosol and nuclear homogenates of HMEC were resolved by polyacrylamide gel electrophoresis, and protein levels were detected by western blot using specific anti-CRT antibody. GAPDH and histone 3 were used as normalization controls. **b** Densitometry was used to quantitate protein levels based from **a**. Statistical significance was measured as standard deviation (SD), and each condition was performed in triplicate ($n = 3$). *#$P < 0.05$ vs. control. **c** The histone acetyltransferase activity of cytosol and nuclear homogenates was detected by the HAT Activity Colorimetric Assay Kit and reflected by the absorbance value at 440 nm. Statistical significance was measured as standard deviation (SD), and each condition was performed in triplicate ($n = 3$). *#$P < 0.05$ vs. control

Fig. 7 The effect of CRT on the ratio of F-actin/G-actin and the acetylation of G-actin of HMEC subjected to MR. **a** The actin stabilization buffer was used to separate soluble G-actin and insoluble F-actin fractions and examined the F-actin/G-actin ratio by Western blotting analysis to assess polymerization/depolymerization of actin in HMEC. The antibody against acetylated lysine was used to detect the acetylation of G-actin fraction. GAPDH was used as a normalization control. **b** Densitometry was used to quantitate protein levels based from the relative expression of F-actin and G-actin. Statistical significance was measured as standard deviation (SD), and each condition was performed in triplicate ($n = 3$). *#$P < 0.05$ vs. control. **c** Densitometry was used to quantitate protein levels based from the relative expression of G-actin and acetylated lysine. Statistical significance was measured as standard deviation (SD), and each condition was performed in triplicate ($n = 3$). *#$P < 0.05$ vs. control. **d** The results of Co-IP to verify the direct interaction between CRT and actin

adhesion, and proliferation. In order to illuminate the effect of CRT pretreatment before MR on cytoskeleton remodeling of endothelial cells, we used the actin stabilization buffer to separate soluble G-actin and insoluble F-actin fractions and examined the F-actin/G-actin ratio by western blotting to assess polymerization/depolymerization of actin in HMEC (Fig. 7a, b). We also used the antibody against acetylated lysine to detect the acetylation degree of G-actin (Fig. 7a, c).

After microwave radiation, compared with control, the F-actin/G-actin ratio of 60 mW group decreased 46% ($P < 0.05$), and the acetylation level of G-actin decreased 20% ($P < 0.05$), while that of CRT + 60 mW group increased 18 and 22%,

respectively ($P < 0.05$). There was statistical difference between 60 mW group and CRT + 60 mW group ($P < 0.05$) (Fig. 7b, c), suggesting that the exogenous CRT pretreatment helps promote G-actin acetylation, upregulate the F-actin/G-actin ratio, stabilize the polymerization status of

microfilaments, and prevent the deacetylation of G-actin and depolymerization of microfilaments induced by MR.

The direct interaction between CRT and actin

Co-IP was used to prove the direct interaction between CRT and actin. In the captured immune complexes of actin, we detected the specific band of CRT. But in the CRT immune complexes, the signal of actin was weak (Fig. 7d). It might be related to the protocol that whole cell lysis (pretreatment with exogenous CRT for 30 min) was used as input sample, and the amount of actin interacting with CRT was too low to be detected by immunoblotting. This primary result gave us the clue of the direct interaction between CRT and actin. In the future, we would use purified proteins of CRT and actin to repeat Co-IP experiments and further verify our hypothesis.

Discussion

Along with the wide applications of microwave in communications, business, medical, and other fields, its health hazards have attracted more and more attention and electromagnetic radiation has been listed as one of the environment hazards that should be controlled by the United Nations Conference on the Human Environment (Pakhomov et al. 1995). The cardiovascular system is one of the most susceptible target organs to microwave radiation (Esmekaya et al. 2011). Our previous work has proved that microcirculature throughout the body is an important target of microwave injury and a key factor affecting the organ damage, repair, and prognosis (Li et al. 2014b). The viability and function of HMEC are essential for microvascular function. The present study showed that along with the increase of microwave power density, the LDH leakage from cells increased, the endothelial migration ability and cell viability decreased, and the continuity of intercellular adhesion molecule VE-cadherin and the arrangement of cytoskeleton stress fiber were destroyed, which indicates that S-band microwave induces dose-dependent injury of human microvascular endothelial cell. This result was similar to those that have been reported in literature (Li et al. 2014a; Xu et al. 2014).

As a multifunctional protein, calreticulin regulates glycoprotein assembly and calcium homeostasis in ER and functions biologically or pathologically as antiapoptosis, phagocytosis, and antigen presentation, etc. in cytosol and nuclei. At present, the effects of CRT on the proliferation and migration of ECs are controversial. It is reported that CRT suppresses tumor growth by inhibiting angiogenesis (López et al. 2010). CRT upregulation is involved in the adaptive response of brain capillary ECs to hypoxia and reoxygenation (Riahi et al. 2010). The adiponectin-CRT/CD91-COX-2 pathway promotes the revascularization after ischemia (Ohashi et al.

2009). Exogenous administration of CRT stimulates nitric oxide generation, promotes endothelial relaxation, and prevents thrombosis (Jeffery et al. 2011). CRT upregulation promotes the degradation of glucose transporter-1 (GLUT-1) mRNA, reduces glucose intake, and inhibits protein glycosylation and free radical formation to prevent diabetic vascular injury (Riahi et al. 2010). Additionally, exogenous CRT enhances wound healing in chronic diabetes by promoting EC migration, proliferation, generation of growth factors, and the phagocytosis of macrophages (Gold et al. 2010). Our previous work proved that before MR, exogenous administration of CRT relieved endoplasmic reticulum stress and protected HMECs (Li et al. 2014a). Overexpression of cytoplasmic calreticulin activated the integrin-FAK signal pathway to alleviate the HMEC injury induced by MR (Xu et al. 2014). This study demonstrates that exogenous CRT reduces LDH leakage from HMEC induced by MR, promotes endothelial migration and cell viability, and maintains the continuity of VE-cadherin and the spatial structure of cytoskeleton.

Cytoskeleton includes microfilament, microtubule, and intermediate filaments. As the important part of cytoskeleton, microfilament skeleton is composed of actin and actin-binding proteins and widely exists in eukaryotic cells. As the major component of the dynamic microfilament system, actin plays essential roles in many cellular activities, such as maintaining cellular structure, promoting proliferation, migration, material transportation, and transmembrane signaling. In live cells, actin has two forms: One of them is G-actin, a globular monomer, and the other one is F-actin, a polymer, which resembles two strings of beads twisted around each other into thin filaments. In the initial stage of polymerization, G-actin is unstable, vulnerable to be degraded by aminopeptidase. But after acetylation of its N-terminal lysine residue, the susceptibility to aminopeptidase reduced. The polymerization capacity and the interaction with myosin of actin increased (Abe et al. 2000; Berger et al. 1981). The acetyltransferases have many different subtypes. Van Damme et al. (2011) mainly focused on the N^{α}-acetyltransferases, which acetylates protein N termini, and reported that γ-actin and β-actin were the most prominent representatives of the group of acidic N termini. Besides the N-terminal acetylation, the lys-50, lys-61, lys-68, lys-191, lys-326, and lys-328 of actin also could be acetylated (Choudhary et al. 2009; Zhao et al. 2010). After the administration of histone deacetylase inhibitor trichostatin A (TSA) in epithelial cell, the deacetylation of actin is inhibited, the content of F-actin increases, and the stress fiber is more stable (Kim et al. 2006). It has been reported that non-muscle or smooth muscle cell cytosolic γ-actin regulates VE-cadherin expression and plays an important role in endothelial cell motility and neovessel maintenance (Pasquier et al. 2015). This work confirms that MR reduces the acetylation level of G-actin and the ratio of F-actin/G-actin, induces cytoskeleton remodeling and stress fiber malalignment, which might be

relevant to cell membrane injury, LDH leakage, intracellular junction damage, and decrease of endothelial migration and viability.

Recently, it is found that calreticulin has acetyltransferase activity, using 7,8-diacetoxy-4-methylcoumarin (Seema et al. 2007) or acetyl-CoA (Singh et al. 2011) as substrates, undergoing autoacetylation to form stable intermediate (Singh et al. 2010), and then transfering acyl group from itself or acetyl-CoA to recombinant glutathione S-transferase (rGST) (Singh et al. 2011). Calreticulin transacetylase (CRTAase) also induces acetylation modification of NADPH cytochrome P450 reductase (Seema et al. 2007), nNOS (Pollard and Cooper 2009), and platelet nitrite reductase, regulating nitric oxide synthesis and preventing platelet aggregation, expression of vascular endothelial growth factor (VEGF), and angiogenesis. The involvement of two lysine residues Lys-173 and Lys-174 present in P-domain for binding acyloxycoumarins and acetyl-CoA highlights that the active site for the CRTAase activity would reside in the P-domain of CRT (Singh et al. 2011). The P-domain of CRT also has the potentional nuclear localization signal as PPKKIKDPD (Michalak et al. 1992). It was reported that nuclear histone H3 lysine (9/14) hyperacetylation appeared to be a potential target of calreticulin transacetylase acetylation system (Verma et al. 2014). Our previous work has confirmed that stresses such as ischemia or hypoxia trigger excessive endoplasmic reticulum stress, disrupt the cytoplasmic Ca^{2+} homeostasis, and induce the overexpression and nuclear translocation of CRT, regulating the gene transcription of ERS-associated apoptosis and aggravating cell injury (Xu and Liu 2015). We also found that pretreatment with exogenous CRT activates the integrin-FAK signal pathway to inhibit gene transcription of apoptosis-associated factors and improve the endothelial function to reduce MR-induced cell injury (Xu et al. 2014). It was reported that a sialic acid-specific lectin from ovine placental cotyledons has the capacity to interact with actin, and the N-terminal sequence of the protein shows 92% identity with rabbit and porcine uterine calreticulin, indicating that CRT might have direct interaction with actin (Iglesias et al. 1996). In the present study, we found that pretreatment of HMEC with CRT prior to MR preserves cytosol CRT content and the activity of HATs, promotes G-actin acetylation, increases the F-actin/G-actin ratio, stabilizes the cytoskeletal stress fiber structure, and at the same time suppresses MR-induced CRT nuclear translocation, inhibiting the acyltransferase activity of nuclear CRT to induce histone lysine residue acetylation and affect gene transcription.

In conclusion, we induced human microvascular endothelial cell injury by MR to investigate the protective effect of exogenous recombinant calreticulin and confirmed that MR induces the power intensity-dependent injury of HMEC. Administration of CRT before radiation preserved the cell viability and exerted cytosol acetyltransferase activity,

catalyzing G-actin acetylation, promoting actin polymerization, stabilizing cytoskeleton structure, maintaining the continuity of VE-cadherin, improving endothelial function, and reducing HMEC injury induced by MR.

References

Abe A, Saeki K, Yasunaga T, Wakabayashi T (2000) Acetylation at the N-terminus of actin strengthens weak interaction between actin and myosin. Biochem Biophys Res Commun 268:14–19 2000

Bender A, Zapolanski T, Watkins S, Khosraviani A, Seiffert K, Ding W, Wagner JA, Granstein RD (2008) Tetracycline suppresses ATP gamma S-induced CXCL8 and CXCL1 production by the human dermal microvascular endothelial cell-1 (HMEC-1) cell line and primary human dermal microvascular endothelial cells. Exp Dermatol 17: 752–760 2008

Berger EM, Cox G, Weber L, Kenney JS (1981) Actin acetylation in drosophila tissue culture cells. Biochem Genet 19:321–331 1981

Choudhary C, Kumar C, Gnad F, Nielsen ML, Rehman M, Walther TC, Olsen JV, Mann M (2009) Lysine acetylation targets protein complexes and co-regulates major cellular functions. Science 325:834–840

Esmekaya MA, Ozer C, Seyhan N (2011) 900 MHz pulse-modulated radiofrequency radiation induces oxidative stress on heart, lung, testis and liver tissues. Gen Physiol Biophys 30:84–89

Gao XF, Wang SM, Peng RY, Gao YB, Li X, Dong HY, Ma JJ (2008) High power microwave radiation damages blood-testis barrier in rats. Zhonghua Nan Ke Xue 14:579–582 (in chinese)

Gold LI, Eggleton P, Sweetwyne MT, Van Duyn LB, Greives MR, Naylor SM, Michalak M, Murphy-Ullrich JE (2010) Calreticulin: non-endoplasmic reticulum functions in physiology and disease. FASEB J 24:665–683

Haseloff RF, Krause E, Bigl M, Mikoteit K, Stanimirovic D, Blasig IE (2006) Differential protein expression in brain capillary endothelial cells induced by hypoxia and posthypoxic reoxygenation. Proteomics 6:1803–1809

Hou G, Xue L, Lu Z, Fan T, Tian F, Xue Y (2007) An activated mTOR/p70S6K signaling pathway in esophageal squamous cell carcinoma cell lines and inhibition of the pathway by rapamycin and siRNA against mTOR. Cancer Lett 253:236–248

Iglesias MM, Cymes GD, Wolfenstein-Todel C (1996) A sialic acid-binding lectin from ovine placenta: purification, specificity and interaction with actin. Glycoconj J 13:967–976

Jeffery E, Peters LR, Raghavan M (2011) The polypeptide binding conformation of calreticulin facilitates its cell-surface expression under conditions of endoplasmic reticulum stress. J Biol Chem 286:2402–2415

K Sri N (2015) Mobile phone radiation: physiological & pathophysiologcal considerations. Indian J Physiol Pharmacol 59: 125–135

Kantz J, Muller J, Hadeler KP, Landstorfer FM, Lang F (2005) Insensitivity of cardiovascular function to low power cm^2/mm-microwaves. Int J Environ Health Res 15:207–215

Kim SC, Sprung R, Chen Y, Xu Y, Ball H, Pei J, Cheng T, Kho Y, Xiao H, Xiao L, Grishin NV, White M, Yang XJ, Zhao Y (2006) Substrate and functional diversity of lysine acetylation revealed by a proteomics survey. Mol Cell 23:607–618

Li QF, Zhao YJ, Fu HM (1997) Effect of microwave radiation and visual display terminal on nailfold microcirculation in human body. Chinese J Microcirculation 7:14–15

Li WH, Li YZ, Song DD, Wang XR, Liu M, Wu XD, Liu XH (2014a) Calreticulin protects rat microvascular endothelial cells against microwave radiation-induced injury by attenuating endoplasmic reticulum stress. Microcirculation 21:506–515

López NC, Valck C, Ramírez G, Rodríguez M, Ribeiro C, Orellana J, Maldonado I, Albini A, Anacona D, Lemus D, Aguilar L, Schwaeble W, Ferreira A (2010) Antiangiogenic and antitumor effects of Trypanosoma cruzi calreticulin. PLoS Negl Trop Dis 4:e730

Michalak M, Groenendyk J, Szabo E, Gold LI, Opas M (2009) Calreticulin, a multi-process calcium-buffering chaperone of the endoplasmic reticulum. Biochem J 417:51–66

Michalak M, Milner RE, Burns K, Opas M (1992) Calreticulin. Biochem J 285(Pt 3):681–692

Ohashi K, Ouchi N, Sato K, Higuchi A, Ishikawa TO, Herschman HR, Kihara S, Walsh K (2009) Adiponectin promotes revascularization of ischemic muscle through a cyclooxygenase 2-dependent mechanism. Mol Cell Biol 29:3487–3499

Pakhomov AG, Dubovick BV, Degtyariov IG, Pronkevich AN (1995) Microwave influence on the isolated heart function: I. Effect of modulation. Bioelectromagnetics 16:241–249

Pasquier E, Tuset MP, Sinnappan S, Carnell M, Macmillan A, Kavallaris M (2015) γ-actin plays a key role in endothelial cell motility and neovessel maintenance. Vasc Cell 7:2. doi:10.1186/s13221-014-0027-2

Pollard TD, Cooper JA (2009) Actin, a central player in cell shape and movement. Science 326:1208–1212

Riahi Y, Sin-Malia Y, Cohen G, Alpert E, Gruzman A, Eckel J, Staels B, Guichardant M, Sasson S (2010) The natural protective mechanism against hyperglycemia in vascular endothelial cells: roles of the lipid peroxidation product 4-hydroxydodecadienal and peroxisome proliferator-activated receptor delta. Diabetes 59:808–818

Sanders AP, Joines WT, Allis JW (1984) The differential effects of 200, 591, and 2,450 MHz radiation on rat brain energy metabolism. Bioelectromagnetics 5:419–433

Secomb TW, Pries AR (2011) The microcirculation: physiology at the mesoscale. J Physiol 589:1047–1052

Seema, Kumari R, Gupta G, Saluja D, Kumar A, Goel S, Tyagi YK, Gulati R, Vinocha A, Muralidhar K, Dwarakanth BS, Rastogi RC, Parmar VS, Patkar SA, Raj HG (2007) Characterization of protein transacetylase from human placenta as a signaling molecule calreticulin using polyphenolic peracetates as the acetyl group donors. Cell Biochem Biophys 47:53–64

Singh P, Ponnan P, Krishnan S, Tyagi TK, Priya N, Bansal S, Scumaci D, Gaspari M, Cuda G, Joshi P, Gambhir JK, Saluja D, Prasad AK, Saso L, Rastogi RC, Parmar VS, Raj HG (2010) Protein acyltransferase function of purified calreticulin, part 1: characterization of propionylation of protein utilizing propoxycoumarin as the propionyl group donor. J Biochem 147:625–632

Singh P, Ponnan P, Priya N, Tyagi TK, Gaspari M, Krishnan S, Cuda G, Joshi P, Gambhir JK, Sharma SK, Prasad AK, Saso L, Rastogi RC, Parmar VS, Raj HG (2011) Protein acyltransferase function of purified calreticulin: the exclusive role of P-domain in mediating protein acylation utilizing acyloxycoumarins and acetyl CoA as the acyl group donors. Protein Pept Lett 18:507–517

Tao T, Wang X, Liu M, Liu X (2015) Myofibrillogenesis regulator-1 attenuates hypoxia/reoxygenation-induced injury by repairing microfilaments in neonatal rat cardiomyocytes. Exp Cell Res 337:234–242

Terman JR, Kashina A (2013) Post-translational modification and regulation of actin. Curr Opin Cell Biol 25:30–38

Van Damme P, Evjenth R, Foyn H, Demeyer K, De Bock PJ, Lillehaug JR, Vandekerckhove J, Arnesen T, Gevaert K (2011) Proteome-derived peptide libraries allow detailed analysis of the substrate specificities of N (alpha)-acetyltransferases and point to hNaa10p as the post-translational actin N (alpha)-acetyltransferase. Mol Cell Proteomics 10:M110.004580

Verma A, Venkateswaran K, Farooque A, Bhatt AN, Kalra N, Arya A, Dhawan A, Arya MB, Raj HG, Prasad AK, Parmar VS, Dwarakanath BS (2014) Cytotoxic and radio-sensitizing effects of polyphenolic acetates in a human glioma cell line (BMG-1). Curr Pharm Des 20:1161–1169

Vicari D, Foy KC, Liotta EM, Kaumaya PT (2011) Engineered conformation-dependent VEGF peptide mimics are effective in inhibiting VEGF signaling pathways. J Biol Chem 286:13612–13625

Wang HT, Lee HI, Guo JH, Chen SH, Liao ZK, Huang KW, Torng PL, Hwang LH (2012a) Calreticulin promotes tumor lymphocyte infiltration and enhances the antitumor effects of immunotherapy by upregulating the endothelial expression of adhesion molecules. Int J Cancer 130:2892–2902

Wang X, Liu X, Wang S, Luan K (2012b) Myofibrillogenesis regulator 1 induces hypertrophy by promoting sarcomere organization in neonatal rat cardiomyocytes. Hypertens Res 35:597–603

Wang X, Tao T, Ding R, Song D, Liu M, Xie Y, Liu X (2014) Kidney protection against ischemia/reperfusion injury by myofibrillogenesis regulator-1. Am J Nephrol 39:279–287

Xu FF, Liu XH (2015) Calreticulin translocation aggravates endoplasmic reticulum stress-associated apoptosis during cardiomyocyte hypoxia/reoxygenation. Chin Med J 128:353–360

Xu FF, Tao TQ, Wang XR, Li YZ, Song DD, Liu M, Liu XH (2014) Cytosolic calreticulin inhibits microwave radiation-induced microvascular endothelial cell injury through the integrin-focal adhesion kinase pathway. Microcirculation 21:717–729

Li Y, Xiaoling Q, Wang X, Liu M, Wang C, Lv Z, Li W, Tao T, Song D, Liu X (2014b) Microwave radiation injuries microvasculature through inducing endoplasmic reticulum stress. Microcirculation 21:490–498

Zhao L, Peng RY, Wang SM, Wang LF, Gao YB, Dong J, Li X, Su ZT (2012) Relationship between cognition function and hippocampus structure after long-term microwave exposure. Biomed Environ Sci 25:182–188

Zhao S, Xu W, Jiang W, Yu W, Lin Y, Zhang T, Yao J, Zhou L, Zeng Y, Li H, Li Y, Shi J et al (2010) Regulation of cellular metabolism by protein lysine acetylation. Science 327:1000–1004